InSAR monitoring of slopes to build back safer

Prepared by: Prof Martin Brook, Dr Matt Cook, Harry Le Cheminant, Wali Akhtar, Sarah Codyre

School of Environment, The University of Auckland

m.brook@auckland.ac.nz

29 June 2026

Acknowledgements

Natural Hazard Commission Toka Tū Ake are acknowledged for funding, as well as School of Environment, University of Auckland for funding and technical support. University of Auckland Centre for eResearch are thanked for providing their advanced computing facilities and for hosting the large datasets produced. Gisborne Council, in particular Dr Murry Cave, are thanked for arranging site access for ground truthing, and for liaising with landowners. Communities of Karekare, Muriwai and Tairāwhiti are thanked for their interest in our studies, facilitating site access and for providing helpful advice for visiting students.

Executive Summary

Annually, landslides cause millions of dollars of damage in Aotearoa New Zealand. Indeed, landslides are prevalent geomorphological features that are observed throughout much of Aotearoa New Zealand, and on the North Island, landslides have proven to be one of the primary landscape-forming processes. Given the mid-latitude, convergent plate margin setting, large parts of the North Island, in particular, are subject to what have been termed multiple occurrence regional landslide events (MORLEs). This is where tens of thousands of landslides can occur across a region over a short timeframe (<24 h), triggered by either an earthquake or a rainstorm, causing fatalities as well as damaging infrastructure and property. Because of such effects, landslides have caused more fatalities than any other natural hazard in Aotearoa New Zealand, since records began.

Indeed, much of Aotearoa New Zealand suffers from landslides for 3 reasons: (1) the terrain is quite steep, (2) the humid (wet) maritime climate, and (3) much of the land surface has been changed by human activities. We have built many of our suburbs on land that has been unstable for centuries, without realising the landslide hazard that exists. A major problem is trying to determine which areas are unstable, because much of the land surface is not monitored by any in situ instrumentation, and slopes are aften moving at only rates of only a few centimetres or millimetres per year. Nevertheless, detecting any changes in slope deformation is important because it can indicate growing land instability.

In situ instrumentation within a slope (e.g. tilt meters, piezometers, extensometers etc) provides low spatial resolution, as the instrumentation may be a local-scale monitoring programme at a borehole in a paddock above a road, or above a house. However, the installed instruments do usually provide data at a high temporal resolution (automatic readings several times per hour). Planning authorities and landowners ideally require slope monitoring data that is (1) spatially extensive (i.e. covers large geographic areas), (2) at a high temporal resolution (annual measurements are not frequent enough), and that provides (3) measurements at ideally mm-scale.

In recent years, emerging technologies include InSAR (Interferometric Synthetic Aperture Radar), which is becoming increasingly important to assess landslides in urban and suburban areas. In Europe, InSAR has shown to be useful in detecting slow-moving landslides, and from this, acceleration of slope deformation in response to rainfall or land use change can sometimes be determined. This is important, because it implies the possibility of using InSAR as part of a landslide early warning system. This would potentially be useful in areas like Gisborne and Auckland, where soil moisture can increase in soils over several weeks of wet weather, leading to tension cracking and eventual large-scale slope failure.

This project used synthetic aperture radar (SAR) from the European Space Agency's Sentinel satellite constellation. These satellites orbit the planet and scan a point on the Earth's surface every 2-3 weeks. When a new scan is compared with the previous scan, the amount that the slope has moved can be determined, even if the movement is as small as a few millimetres. This precision is possible due to several reasons. With persistent scatter (PS) processing used here, only points of high coherence were used. Coherence represents the confidence level (0 to 1) of each pixel in the phase difference image. Low coherence (<0.2) often indicates phase noise and higher uncertainty, so the low coherence points (<0.2) were removed during processing. E-InSAR (enhanced InSAR) which combined PS and SBAS (small baseline subset) was applied to the Gisborne region. This identified long-tern slope movements, shrink-swell of clay rich soils, as well as toe uplift.

In our study, movement was detected in all of our study areas (Muriwai and Karekare in Auckland; suburban Gisborne), but it varied markedly in time, and within each study area. Increased rainfall allowed slopes to speed up for a short period of time. Asecondary finding relates to the annual cycle of shrinking and swelling of soils. In winter, the wetter conditions cause soils to expand, and then drying in the summer causes soils to shrink. This was also detected using the satellite radar. These results might be useful in determining requirements for foundation design for houses. The more seasonal shrinking and swelling of soils, then the more steel reinforcement is required in concrete slab foundations, for example.

Abstract

This study focuses on the steep, unstable slopes in the Waitākere Ranges, at Muriwai and Karekare to the west of Auckland, as well as the Gisborne area of the east coast. Typical slope failures in these area are shallow landslides, that are typically initiated by intense rainfall, following prolonged wet periods. These landslides are usually in soils and sometimes include the underlying highly weathered rock. This study uses Interferometric Synthetic Aperture Radar (InSAR) analysis of Sentinel-1 imagery to explore the pattern of ground deformation in the selected slopes. In Karekare and Muriwai, the InSAR timeseries of data was between July 2022 and July 2024. In the Gisborne area, the InSAR timeseries was July 2021 to July 2025. To enhance the interpretation of the InSAR results, regional LiDAR data, aerial imagery, and field mapping of landslide features were also used in order to validate InSAR displacement patterns and to delineate areas of slope deformation. Despite some noise in the InSAR displacement data, coherence was high, and the results were sufficient to detect some unstable slopes across the study areas. At Karekare and Muriwai, as well as the Gisborne region, deformation is primarily associated with slow creep and shallow landslides. Major inflections in data occur around the Cyclone Gabrielle event. Nevertheless, many slopes show ongoing pre- and post-Gabrielle deformation. A further seasonal cycle of deformation identified relates to shrinking and swelling of clay-rich soils. This lower amplitude deformation can be delineated at many sites, and may cause longer-term strain softening of these surface materials. Understanding the relationships between antecedent rainfall and rainfall event intensities may in future provide insights into relationships between rainfall thresholds and slope deformation. The implication is that InSAR may prove to be a suitable tool within a landslide early warning system in Aotearoa New Zealand, in future. This research demonstrates how satellite-based monitoring could support more resilient hazard management. A broader adoption of InSAR embedded within land-use planning, would enhance the ability to identify at-risk slopes and reduce hazard exposure, thereby supporting safer, more resilient communities.

Keywords

Landslide, InSAR, Monitoring, Rainfall, Quantifying hazards and risk

Introduction

Since 2019, a series of high intensity rainfall events occurred across many regions of Te Ika-a-Māui, in particular the Tairāwhiti region (Despojo et al., 2025). In each case, this has led to multiple occurrence regional landslide events (MORLEs; Brook, 2023). Sometimes, the rainfall event has been a fast-moving ex-tropical cyclone, and in other cases the storm has been slow-moving and of lesser intensity, but its effects have been substantial due to being preceded by several weeks of wet weather, thus developing high antecedent soil moisture conditions (Pola et al., 2025; Abazu et al., 2025; Howard et al., 2025; Brook and Nicoll, 2024).

Concern has been growing among researchers that this damaging pattern of rainstorms is driven by climate change. Indeed, only two weeks prior to the arrival of ex-Tropical Cyclone Gabrielle in February 2023, Aotearoa New Zealand experienced its costliest ever extreme rainfall event in the form of the Tāmaki Makaurau Anniversary weekend floods (Brook and Nicoll, 2024). This rain event brought widespread devastation to Te Tai Tokerau but particularly across Tāmaki Makaurau, the largest city in the country. Earlier in January, Cyclone Hale also resulted in significant rainfall across many regions of Te Ika-a-Māui. In fact, it was the wettest January on record for nearly all locations in Te Ika-a-Māui which were subsequently impacted by ex-Tropical Cyclone (TC) Gabrielle. Event attribution studies of TCs provide evidence of increased rainfall associated with anthropogenic influence (IPCC AR6). Event attribution is the extent to which human activities have influenced a specific weather event, by assessing how much climate change has increased the likelihood or intensity of the weather event. Thus, it is now imperative that we develop an understanding of where slopes are most vulnerable to rainfall-induced failure, and identify any other anthropogenic factors (e.g., land use changes) that can exacerbate the effects of rainfall on slope instability.

The research highlighted herein builds on the preliminary Interferometric Synthetic Aperture Radar (InSAR) monitoring of landslides work that members of the team completed in Tairāwhiti in recent years, until the end of 2021. That investigation formed the basis of the PhD recently completed by Matt Cook. As a proof of concept, we determined that the Sentinel-1 InSAR data could be used to analyse mm-scale slope deformation in the region. Indeed, Matt Cook wrote the computer code that can be used to "decipher" the raw satellite radar returns, and turn the data into slope movement information, critical for end-user decision-making. The results were published in a series of journal articles co-authored by Matt Cook and Martin Brook, with digital output provided to Gisborne District Council (Cook et al., 2022a,b,c; 2023a,b).

Thus, the aim is to identify landslides spatially, and delineate temporally, (1) when, (2) why (i.e. what is the process triggering slope movement), and (3) at what rate the slopes have been deforming, and this will be applied to the last several years.

Methodology

Large-scale landslide events such as MORLEs trigger thousands of slope failures simultaneously within short time frames, which makes it extremely difficult to monitor using site-specific conventional ground-based methods like extensometers or inclinometers. Because of the necessity to do so, there has been a growing reliance on remote sensing technologies such as UAV surveys, LiDAR, and InSAR, which are now recognised as crucial/essential tools for landslide recognition, deformation monitoring, and hazard assessment (Solari et al., 2020).

Interferometric Synthetic Aperture Radar (InSAR) is an active remote sensing technique growing in popularity within the scientific community, specifically for geotechnical and geohazard research to monitor ground surface deformation and generate Digital Elevation Models (DEMs) (Cook et al., 2023a). This technique measures the phase difference between two or more radar images acquired over the same location at different times, enabling the detection of subtle horizontal and vertical ground displacement with centimetre to millimetre-scale accuracy (Ferretti et al., 2014).

InSAR works by “transmitting microwave radar signals from a satellite or airborne platform to the Earth’s surface” and recording the reflected signals. The term “synthetic aperture” essentially refers to the enlargement of the antenna by combining radar echoes from successive positions along the satellite's orbit (Cook et al., 2023a). By combining returns from multiple positions along the satellite’s orbit, the spatial resolution and image quality can be enhanced, allowing for detailed ground deformation monitoring (Ferretti, 2014; Cook et al., 2023b).

The initial phase involved a desktop review of the high-resolution satellite and aerial imagery data available from Land Information New Zealand’s Data Service (https://data.linz.govt.nz/), facilitating the development of preliminary geomorphic maps. Following the desktop phase, field-based geomorphic mapping was undertaken by visual inspection of landslides at the sites. These observations were subsequently integrated with LiDAR digital elevation models (DEMs) to validate and refine the landslide inventory, highlighting elevation change and assessing volumetric displacement. Geospatial analysis was undertaken in ArcGIS Pro to extract terrain metrics and identify features indicative of mass movement in relation to six primary topographic parameters, alongside DEM-differencing. InSAR (Interferometric Synthetic Aperture Radar) time-series analysis was then employed to assess the cumulative ground deformation patterns.

Specifically, this study utilised InSAR data acquired from the Sentinel-1A satellite and adopted the Persistent Scatterer InSAR (PS-InSAR) approach for the time series analysis. PS-InSAR is part of a broad group of time series InSAR techniques that rely on stable, long-term coherent targets, typically man-made structures (e.g., buildings, bridges, infrastructure), or exposed rock surfaces (Hooper, 2008; Yunjun et al., 2019; Cook et al., 2023a,b). This method is particularly well-suited to suburban environments, where these stable targets are more common.

The methodology is separated into four main stages as follows: (1) Data acquisition and initial Sentinel-1 SAR data preparation using Single Look Complex (SLC) format, (2) using SARscape for interferogram generation involving processing SAR image pairs to produce a stack of unwrapped interferograms, (3) time series analysis applying the PS-InSAR approach in SARscape software to detect and quantify ground displacement over time, (4) post-processing and visualisation of time series deformation maps and exporting the results for analysis. Figure 1 shows an example flow diagram of how the methods where applied for the Auckland sites (Muriwai and Karekare). The same approach was taken for Gisborne.

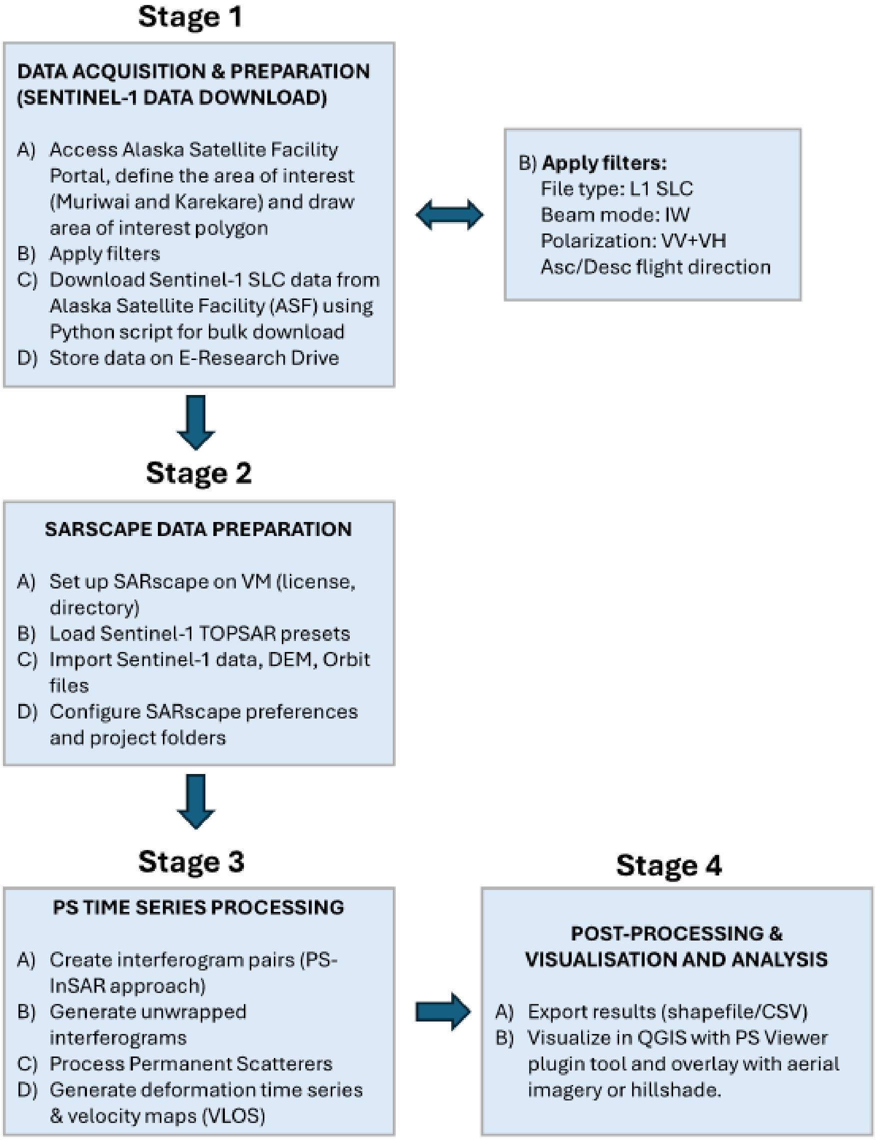

Figure 1: InSAR (e.g. PS time series) methodology workflow implemented to generate interferograms and time series displacement analysis using SARscape and QGIS software.

This research focused on the use of Sentinel-1 datasets sourced from the Alaskan Satellite Facility (ASF) Vertex portal within the wider European Space Agency's Copernicus Data Space Ecosystem (https://search.asf.alaska.edu/#/). Sentinel-1 captures data across 250-kilometre-wide swaths with an approximate spatial resolution of 5 metres in the east-west direction and 20 metres north-south, by using the Terrain Observation in conjunction with the Progressive Scans SAR (TOPSAR) technique.

SAR images acquired in both descending orbits were used for the analysis. The Sentinel-1 data were processed using Single Look Complex (SLC) images for the interferogram generation and time series analysis. As an example, for Auckland, the descending dataset includes 59 acquisitions from track 146, frame 716, which were obtained between 5 July 2022 and 6 July 2024 to support complementary analysis. A summary of the interferogram stack generation for both datasets is provided in Table 1.

Table 1: Summary of the Sentinel-1 SLC SAR images used to generate interferograms results.

Satellite	Orbit Geometry	Track no.	Frame no.	Sub-swath	No. of Acquisitions	Acquisition period
S1A/S1C	Descending	146	716	2	59	05/07/2022 to 06/07/2024

All PS-InSAR displacement and velocity results presented in this study are expressed relative to a stable spatial reference point from each area. The key steps for the PS-InSAR processing are outlined as follows.

- Co-registration of all SAR images to a selected master file
- Interferogram generation for each pair
- First Inversion, estimating residual height and linear displacement velocity
- Second Inversion, removing atmospheric phase delays and refining estimates
- Geocoding, converting results into geographic coordinates for interpretation

The outputs for this stage include a displacement time series for each PS point, followed by velocity in the line-of-sight (VLOS) maps, and quality layers used in subsequent post-processing analysis and visualisation stage. This step is crucial for the identification and monitoring of ground deformation such as subsidence or slow-moving landslides.

In order to understand the line-of-sight velocity, Cook (2023b) explains that negative values typically indicate movement away from the sensor (downslope), while positive values reflect movement toward the sensor, which could suggest uplift or uphill creep (Cook et al., 2023b). The accuracy of these interpretations depends on coherence, which is calculated based on the alignment between the slope and the sensor's line of sight (LOS) in the north, east, and vertical directions. Low coherence values can reduce reliability and may result in inaccurate VLOS readings (Cook et al., 2023b).

Time-series PS-InSAR analysis was conducted relative to a reference image selected near the temporal mid-point of the datasets. For example, for both Muriwai and Karekare study areas this was 12 July, 2023. The selection of a mid-period reference image minimises temporal baselines across the interferogram network.

In addition to the temporal reference, PS-InSAR displacement measurements are spatially related and were referenced to stable persistent scatterer points assumed to represent zero deformation over the monitoring period. As an example, at Muriwai, the reference point (PS28) is located at 22 Motutara Road (WGS84: 174.441° E, -36.821° N), situated outside the landslide areas and exhibiting negligible temporal displacement. At Karekare for example, the reference persistent scatterer corresponds to Point ID7748 at 8 Watchmans Road (WSG: 174.478° E, -36.984° N).

As outlined above, a key concept in InSAR data quality and certainty and confidence in the results, is coherence (C). The coherence is a measure of the similarity in phase between the two SAR acquisitions and is measured on a scale from 0 to 1 (calculation in Notti, 2014). A coherence value of 1 means identical phase values between the images, but a value of 0 means there is decorrelation (Notti, 2014). In InSAR processing, it is apparent that only certain areas exhibit high coherence values, such as buildings and exposed rocks, while areas with high vegetation and bodies of water produce low values (Ferretti, 2014). Data with coherence of $-0.2<C<0.2$ are removed, following Notti (2014). The degree of coherence can be used as a quality measure because it significantly influences the accuracy of the phase differences and height measurements. Coherence is an indicator of the level of noise in the phase of the interferogram pixel. Thus, higher coherence (C) values toward 1 indicate increasing quality of the data. Coherence values for this study are generally high (toward 1), with an example shown in Table 2. The calculation of coherence is shown in Cook et al. (2023b, p. 431) and an explanation is presented in Appendix 1.

Table 2: Example coherence values (C) for Cluster 1, Muriwai.

Point ID	Coherence	Longitude	Latitude	Total movement (mm) 7/6/2024
606	0.789	174.4310508	36.83804036	-28.4
607	0.855	174.4304304	36.83789351	-11.8
615	0.864	174.4310035	36.83816131	-27.9
625	0.777	174.4309768	36.83828714	-26.3

In addition to the Persistent Scatter InSAR processing outlined above, enhanced InSAR ("E-InSAR", SARScape, 2025) processing methodology was also applied, to the Gisborne area only. This method combines both PS-InSAR with SBAS (small baseline subset InSAR), into what is usually termed "E-SBAS" InSAR. Note that SBAS on its own has been used in Gisborne successfully in the past for 2016-2021 (e.g. Cook et al., 2023b). However, as Hussain et al. (2025) have outlined, using processing steps that combine elements of PS-InSAR and elements of SBAS InSAR, can often provide a more useful dataset.

Indeed, PS-InSAR offers high-precision monitoring at the mm-scale, making it highly effective for early warning of landslide disasters (Hussain et al., 2025). In particular, PS-InSAR is useful for long-term monitoring of stable and slow-moving landslide, as it focuses on highly coherent scatterers that remain stable over time. PS-InSAR performs time-series deformation analysis on these stable reflectors at the pixel resolution, providing detailed insights into deformation patterns (Hussain et al., 2025). However, PS-InSAR has two main limitations:

1. In regions where deformation sometimes is more rapid, PS points are sparse, which can lead to a lack of deformation information
2. The reliance of PS-InSAR on stable scatterers means that coverage can be limited in areas where these scatterers are not abundant

In contrast to PS-InSAR, SBAS-InSAR provides relatively uniform time-series points across a landslide region, creating good geographic coverage for the calculation of deformation (Hussain et al., 2025). Also, it can extract a higher density of time-series points compared to PS-InSAR. This is useful for deformation analysis for (1) regions where landslides may be smaller, or (2) where the landslide is a large landslide 'complex' (e.g. Hungr et al., 2014), with sub-areas of secondary landslides within the landslide complex only active at different points in time. However, SBAS-InSAR also has its drawbacks, principally:

1. The spatial multi-look process in SBAS decreases pixel resolution, which can lead to loss of high-quality scatterer signals
2. It also relies on short temporal baselines, which may limit its applicability in certain scenarios where longer baselines are necessary (very slow-moving landslides for example, at 2 mm/ year where deformation phase is tiny, and it may be buried in atmospheric noise)

Table 2 summarises the main advantages and disadvantages of PS-InSAR and SBAS-InSAR. Therefore, each method fills the other's gaps. PS-InSAR provides extremely accurate measurements on stable reflectors. SBAS-InSAR provides much better spatial coverage across areas lacking persistent scatterers. Combining both the methods provides:

- greater spatial coverage,

- higher precision where PS points exist,
- more robust deformation estimates,
- better temporal consistency.

The combined InSAR product often consists of high-precision PS measurements, SBAS measurements over distributed scatterers, one unified deformation time series. The new E-SBAS technique identifies and process Permanent Scatterers (PS) pixels together with Distributed Scatterers (DS) ones, providing a more comprehensive and valuable output. E-SBAS is capable of measuring non-linear displacement trend to both PS and DS pixels. The approach for E-SBAS is inspired by (Lanari, 2004). The deformation products obtained exploit a combination of both Small Baseline subset (SBAS) and Persistent Scatterers (PS) interferometry methods, in order to estimate the temporal deformation at both DS and point-like PS.

Table 2: SBAS-InSAR (Small Baseline Subset InSAR) and PS-InSAR (Persistent Scatterer InSAR) - how they differ and why integration (as "E-SBAS" InSAR) is useful.

PS-InSAR	SBAS-InSAR
Uses highly coherent, stable point targets (buildings, rock outcrops, infrastructure).	Uses interferograms with small spatial and temporal baselines to maximize coherence over distributed areas.
Excellent precision (often millimeter-level).	Better spatial coverage, especially in natural terrain.
Performs best in urban or rocky environments.	Performs well in vegetated and rural regions where coherent pixels are less persistent.
Sparse measurements.	Denser measurements but generally slightly lower precision.

Results and Discussion

Muriwai PS-InSAR

Example results for Muriwai are shown in Figure 2, and the PS-InSAR time-series analysis identified four main persistent scatterer (PS) clusters across Muriwai. Cluster 1, located at 99 Waitea Road and shown in Figure 45A/B, records the largest downslope displacements of all clusters. Cluster 2, situated immediately downslope at 93 Waitea Road, shows intermediate but still notable downslope deformation.

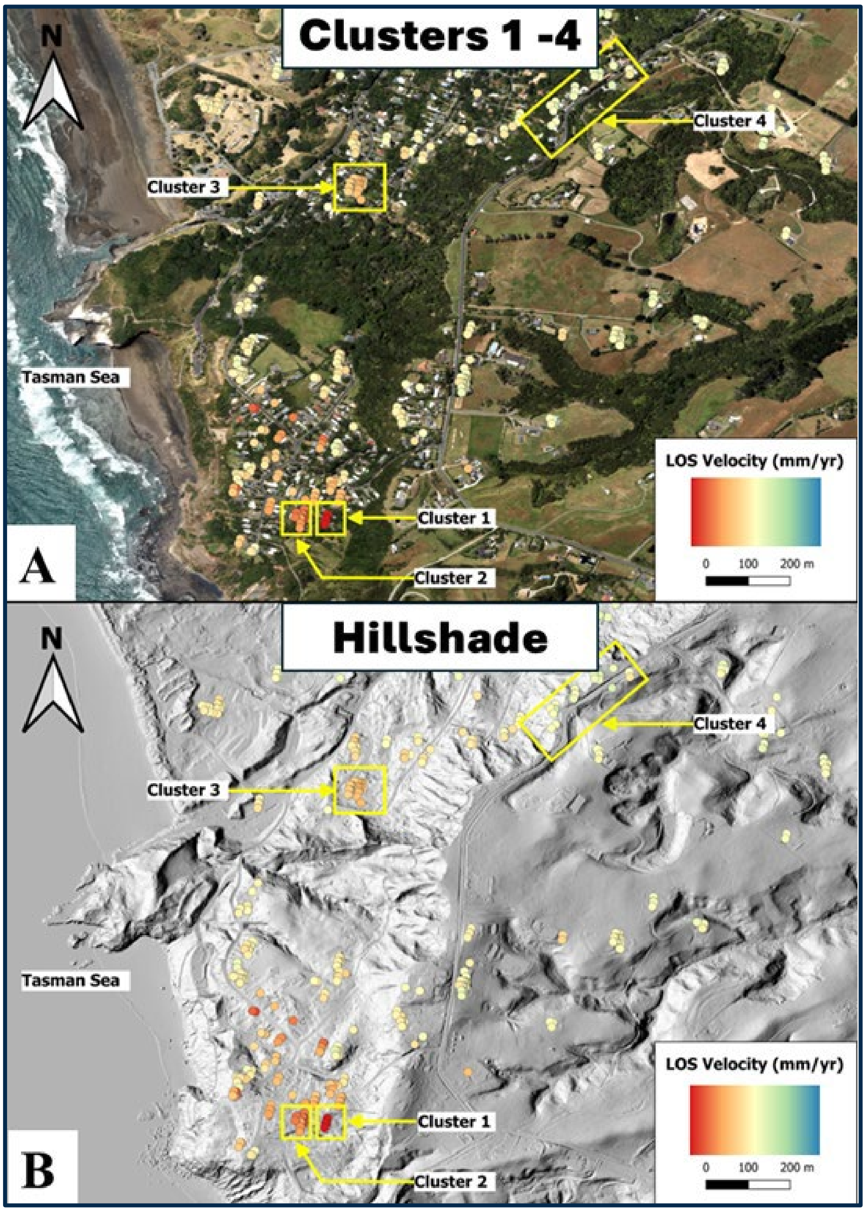

Figure 2: (A) aerial map and (B) hillshade map of PS-InSAR for Muriwai, with four clusters (1-4), monitoring period (5 July 2022 to 6 July 2024).

Cluster 3, located along Domain Crescent, exhibits relatively subdued behaviour. Scatterers here record cumulative displacements from -12.3 mm to -2.7 mm, with velocities generally between -4.9 and -2.1 mm/yr. Minor fluctuations appear during wetter months in 2023, though values remain within natural variability and do not indicate significant creep. In contrast, Cluster 4 situated above the Oaia Road escarpment shows the most stable conditions observed.

Figure 3 shows example InSAR data from Cluster 1, plotted against rainfall. Figure 3(A) shows PS-InSAR hillshade zoomed-in map of Cluster 1, located adjacent to 99 Waitea Road, Muriwai, illustrating paleo-landslide headscarps.

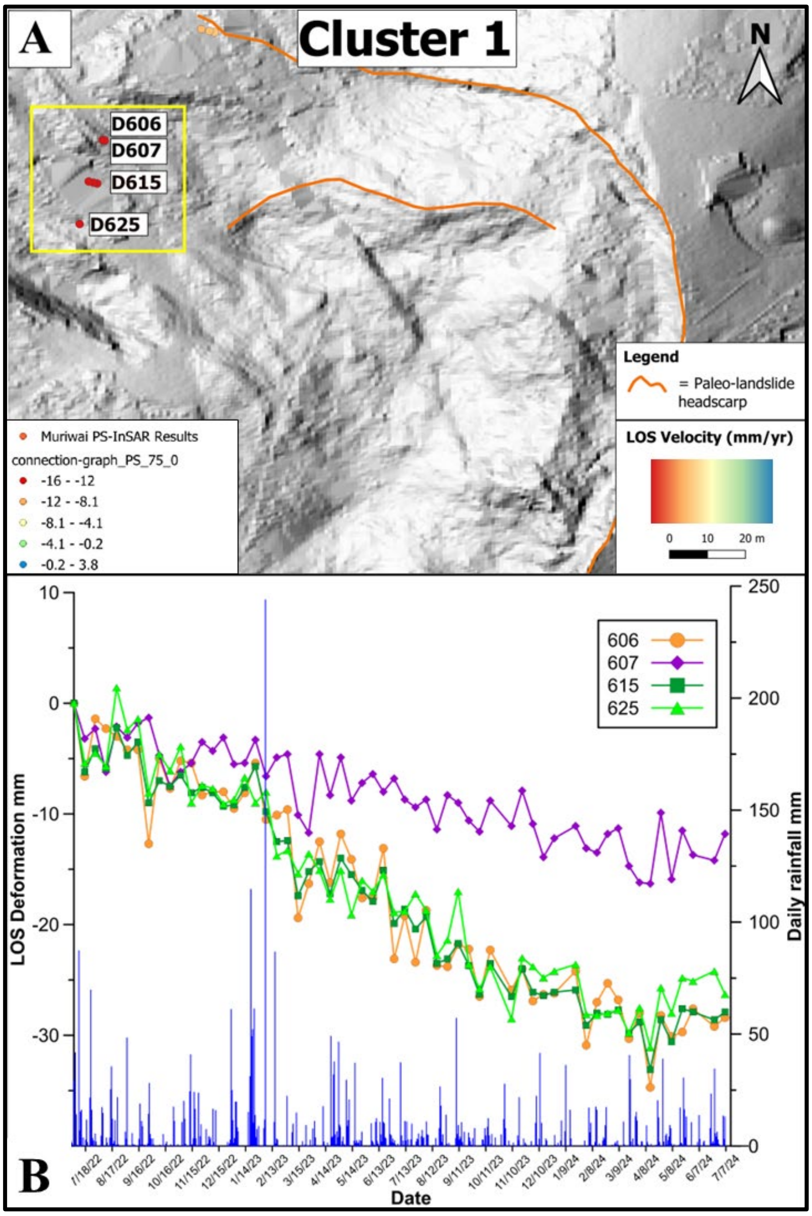

Figure 3: (A) Hillshade of cluster 1 showing paleo landslide headscarps (red); (B) LOS velocity plotted against daily rainfall.

Figure 3(B) shows line of sight (LOS) velocity (mm/yr) time-series deformation plotted against daily rainfall. Cluster 1 records the largest displacements of all identified clusters, with cumulative values ranging from -28.4 mm to -11.8 mm over the two-year monitoring period (5 July 2022 to 6 July 2024).

Further example results for Muriwai (cluster 2) are given in Figure 4. The time-series plots illustrate that movement was not uniform over time. In particular, during late January to early February 2023, displacement steps coincided with the Auckland Anniversary Floods and Cyclone Gabrielle.

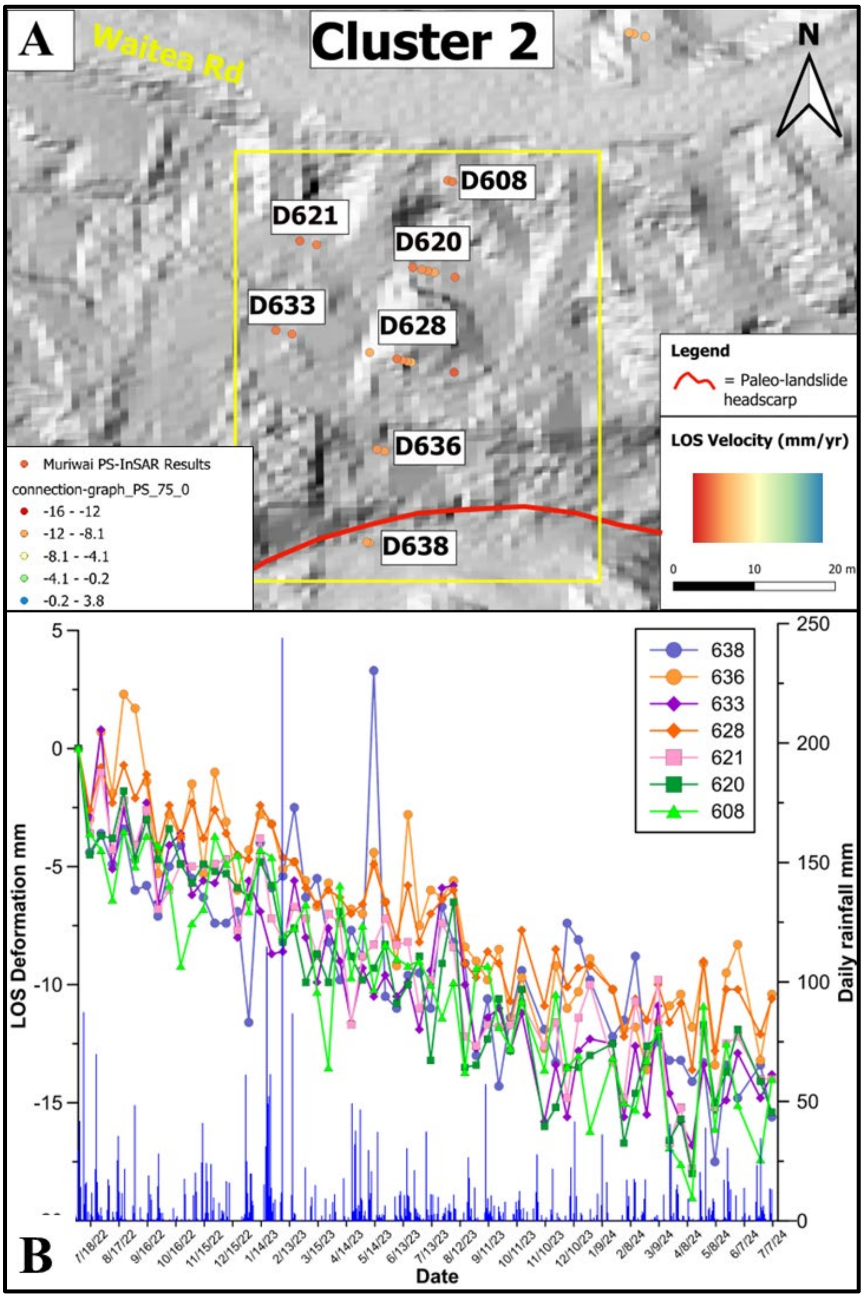

Figure 4: (A) PS-InSAR hillshade of Cluster 2, located adjacent to 93 Waitea Road, Muriwai; (B) Line-of sight (LOS) velocity (mm/yr) time-series deformation plotted against daily rainfall.

For example, PS 618 recorded a downslope shift of -6.3 mm between 25 January and 6 February 2023 (Figure 4B). Cluster 2 reflects steady downslope deformation with a relatively consistent pattern across scatterers; however, the rainfall-linked displacements during early 2023 emphasise that short-term storm events were sufficient to accelerate movement, superimposed on a background of slow creep.

Karekare PS InSAR

For Karekare, 4 clusters were identified (Figure 5), and example InSAR plots are shown in Figure 6 and 7 below.

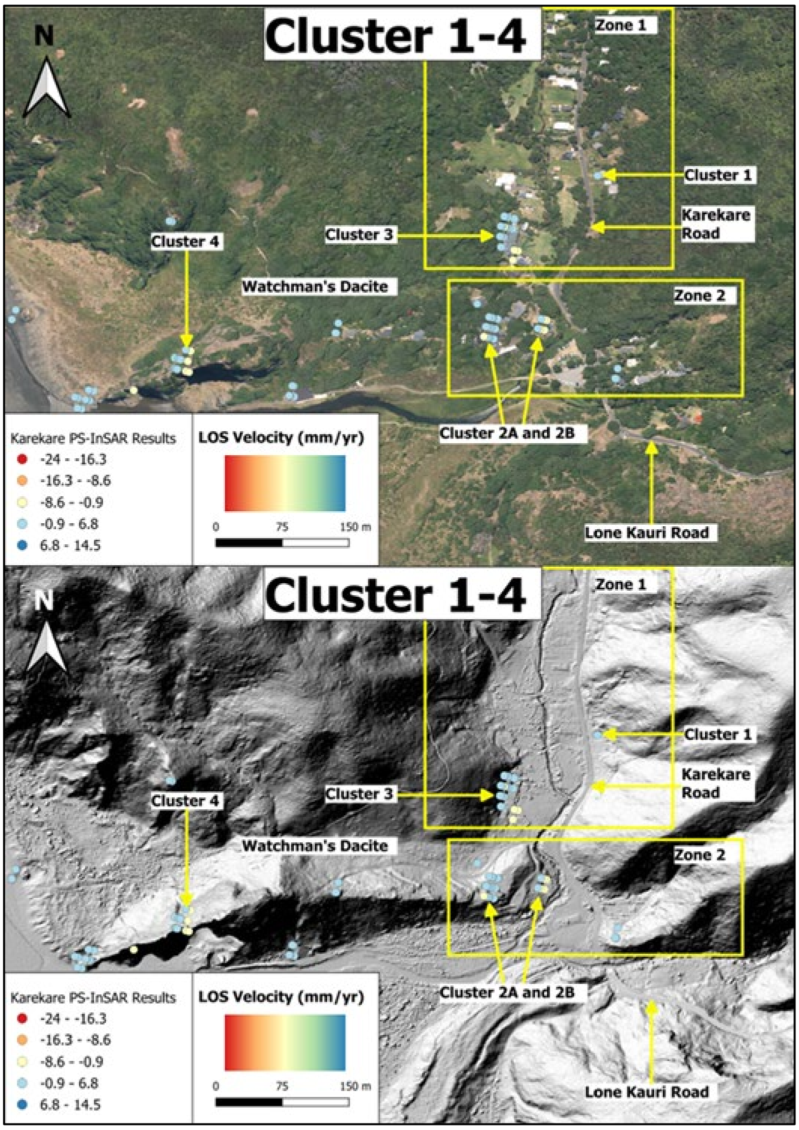

Figure 5: (A) PS-InSAR 0.075 urban aerial map of Karekare (2024-2025); (B) hillshade map of Karekare. Both A and B highlight the four predominant clusters (Cluster 1, Cluster 2A/2B, Cluster 3, and Cluster 4). Cumulative displacements range from 11.6 mm in Cluster 2A (PS 77604) to -15.0 mm in Cluster 4 (PS 77735) over the two-year monitoring period (5 July 2022 to 6 July 2024).

Cluster 1, located within Zone 1 adjacent to 23 Karekare Road, is represented by a single scatterer that shows only minor downslope movement, with a displacement rate of -1.1 mm/yr and cumulative movement of -6.3 mm. In contrast, Clusters 2A and 2B situated on the lower terraces west of Karekare Road (Zone 2) display contrasting behaviour for example, Cluster 2A indicates mild uplift/heave with cumulative displacements up to 11.6 mm, while Cluster 2B records downslope creep of approximately -4 to -5 mm.

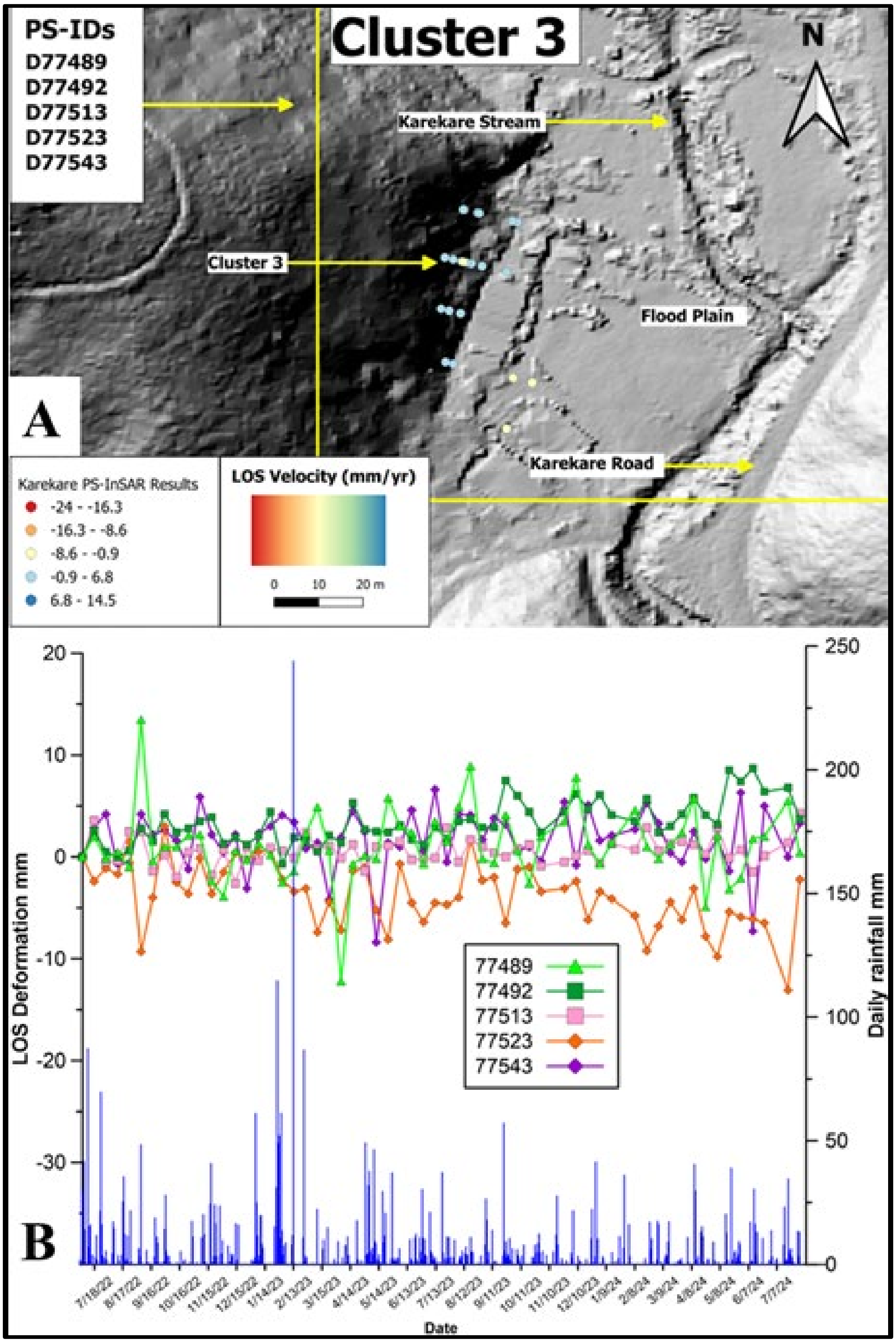

Figure 6: Cluster 3 (A) PS-InSAR hillshade zoomed-in map of Cluster 3, situated within Landslide Zone 1 and adjacent to 1 and 12 Karekare Road, Karekare. (B) Line-of-sight (LOS) velocity (mm/yr) timeseries deformation plotted against daily rainfall for representative scatterers.

Further north along Zone 1, adjacent to 1 and 12 Karekare Road, Cluster 3 demonstrates subdued displacement, with scatterers largely stable and cumulative values between -2.2 mm and 4.3 mm. In comparison, Cluster 4, situated on the steep Watchman Dacite headland, situated west of Zones 1 and 2, shows the most pronounced downslope movement at Karekare, with scatterers averaging -2.7 mm/yr and cumulative values ranging from -15.0 mm to -2.4 mm.

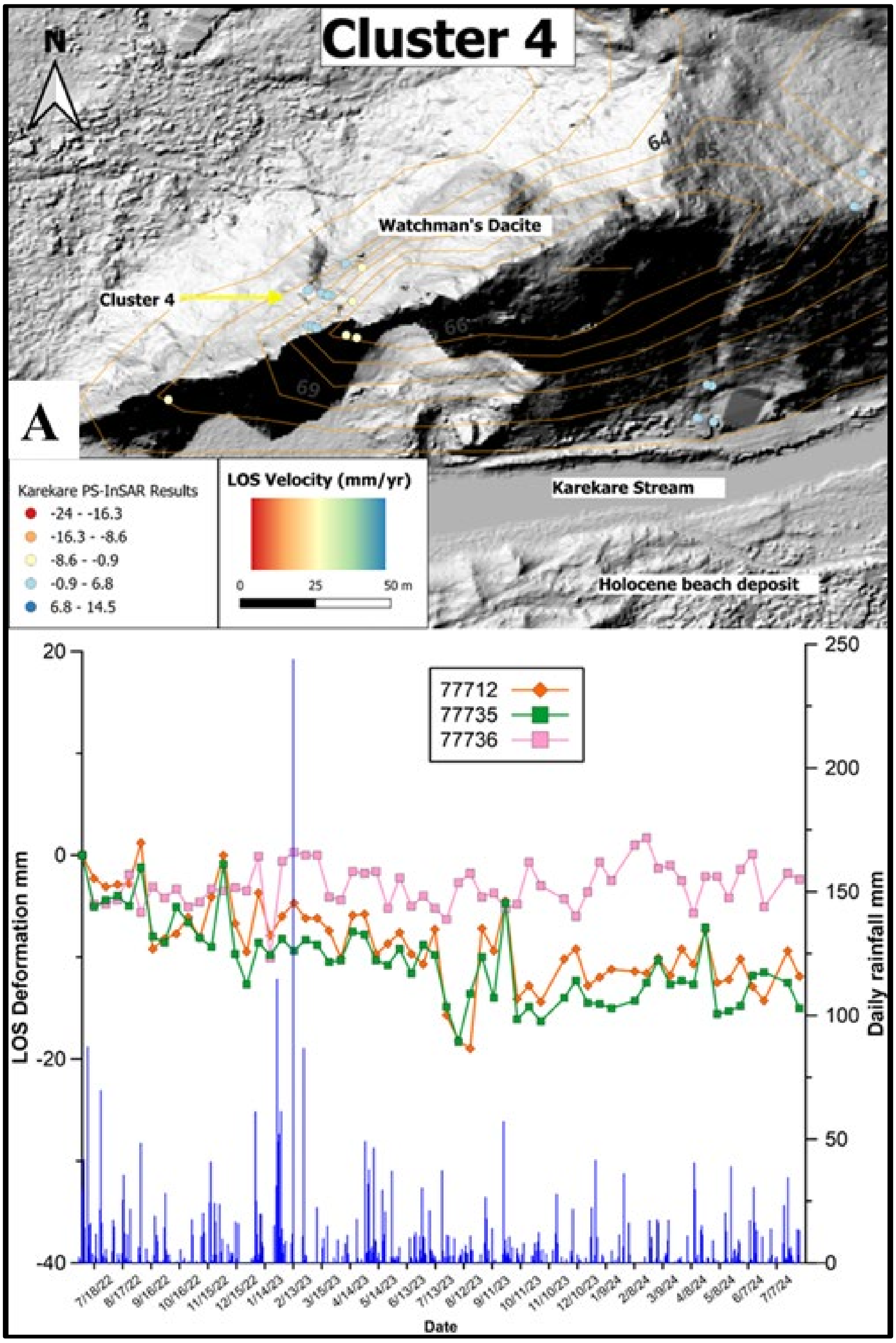

Figure 7: Cluster 4. (A) PS-InSAR hillshade map of Cluster 4, located on the Watchman Dacite headland west of Zones 1 and 2, Karekare. (B) Line-of-sight (LOS) velocity (mm/yr) time-series deformation plotted against daily rainfall.

PS-InSAR results across Karekare indicate slope deformation is generally subdued, with only small-scale slow creep movement observed, as well as seasonal fluctuations in deformation correlating with variability in soil moisture content, causing shrink-swell in expansive residual soils. Cluster 1, represented by a single scatterer at 23 Karekare Road, shows minor downslope movement of -6.3 mm. In contrast, Cluster 4 on the steep Watchman Dacite headland demonstrates the clearest downslope creep, with cumulative displacements of up to -15.0 mm and rainfall-linked steps during early 2023.

These results highlight the contrast between stable slopes within residential areas and the more sensitive dacitic headland, where movement is more strongly expressed.

Gisborne Combined SBAS and PS-InSAR ("E-SBAS" InSAR)

As outlined in the Methods section, for the Gisborne area, an enhanced InSAR method (E-InSAR), that combines both PS and SBAS InSAR (e.g. Hussain et al., 2025; SARScape, 2025) was applied. This was applied over a 5-year period (July 2021 to July 2025), because of the severe storm events from 2021 onwards in the Tairawhiti district. Thus, the 2 years either side of the 2023 storm events provide the opportunity to detect any post-storm acceleration in slope movement. A selection of examples from 4 different areas across Gisborne, are included in the following pages. These show a summary of the types of slope movement that have been detected.

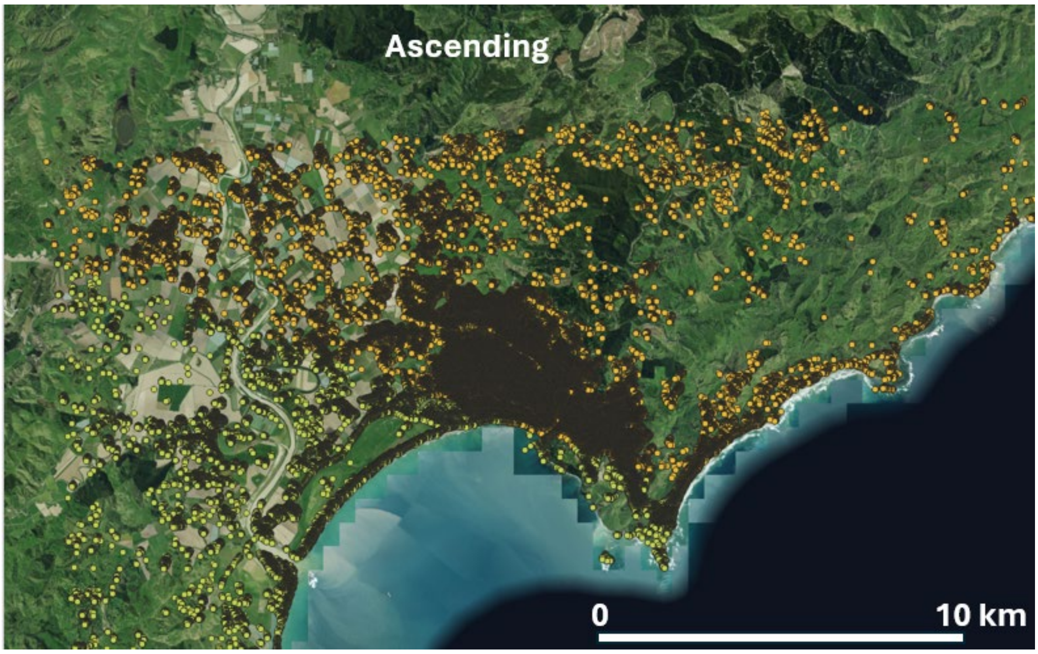

Figure 8: Enhanced (E-InSAR) coverage of Gisborne, combining PS and SBAS. This is for Ascending (i.e. south-north) satellite sensor acquisition.

Wheatstone Road - continuous down-slope movement 2021-2025

Figure 9 shows the Wheatstone Road area to the east of Gisborne CBD. This is an area that has exhibited slope movement in the past on both sides of the valley. The slope identified in this example is on the east-facing slope below 79 Wheatstone Road. The slope is in weathered mid-Miocene age Tolaga Gp mudstones/sandstones, of the Tunanui Fm.

From the points highlighted in Figure 9B&C, there are several important points that are evident. First, considerable slope movement is occurring on this slope at both points. Second, this slope movement follows a rather linear pattern for the 2021-2025 timeseries. Third, there is no evidence of increased acceleration following the storms of early 2023. Indeed, the deformation has continued at a somewhat steady line of sight (LOS) velocity as seen prior to 2023. A EQC claim was settled in for a storm/flood event on 30 July 2012, and this perhaps indicates the long-term issues with steep sites on weathered Tunanui Fm soils.

Oswald Street slopes - segmented hillslope deformation 2021-2025

Figure 10 shows the slopes above the eastern ends of Oswald Street, Gisborne. The yellow arrow in Figure 10A highlights field evidence of a bulging mid-slopes in the area below 1 Oswald Steet. The top of the slope on which 1 Oswald Street is built is on Pleistocene Mangatuna Fm gravels, which are permeable and free-draining. Points 450121 and 448733 are on the underlying Late Miocene Tolaga Gp mudstones.

The slope on which the points are located is deforming, but this deformation is partitioned (or segmented) within the slope. For example, Figure 10B shows point 450121 and this is rather stable, with the pattern of velocity indicating seasonal shrink swelling of the mudstone-derived soils.

In contrast, 15 m to the south, point 448733 shows that significant deformation is occurring within the slope, while some evidence of seasonal shrink-swell is also present (Figure 10C. Of note at point 448733 is also an inflection coinciding with Cyclone Gabrielle in 2023 (blue arrow on plot). However, this shown apparent upward movement (i.e. heave).

Interestingly, a landslip event on 11 June 2014 led to an EQC claim being settled for 1 Oswald Street. The visual evidence (bulging mid-slope) along with the E-InSAR indicates parts of the slope immediately below 1 Oswald Street are still undergoing long-term movement.

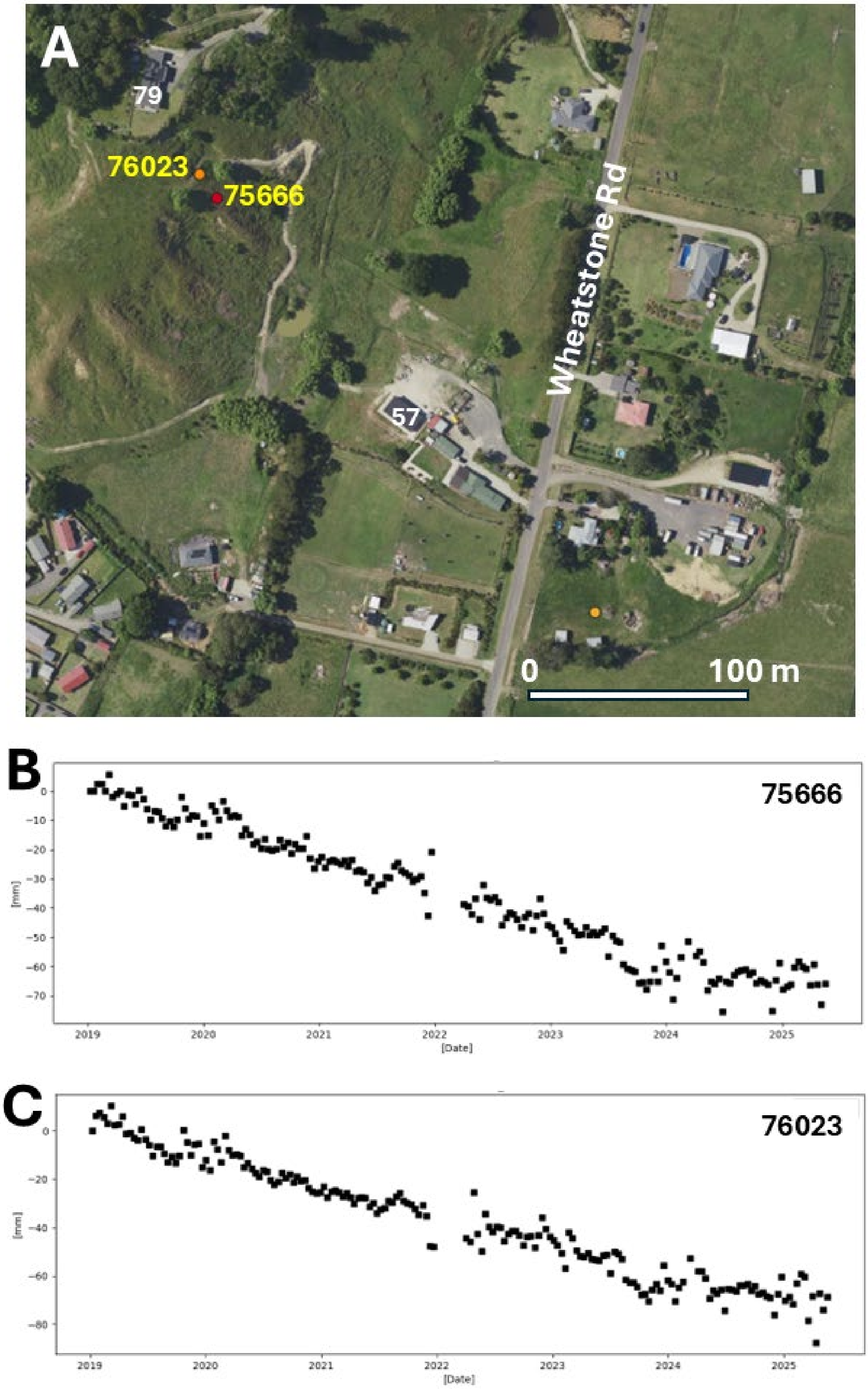

Figure 9: (A) Wheatstone Road area; (B) Line-of-sight (LOS) velocity (mm/yr) time-series for point 75666; (C) Line-of-sight (LOS) velocity (mm/yr) time-series for point 76023. Both points show consistent, downslope movement toward Wheatstone Road.

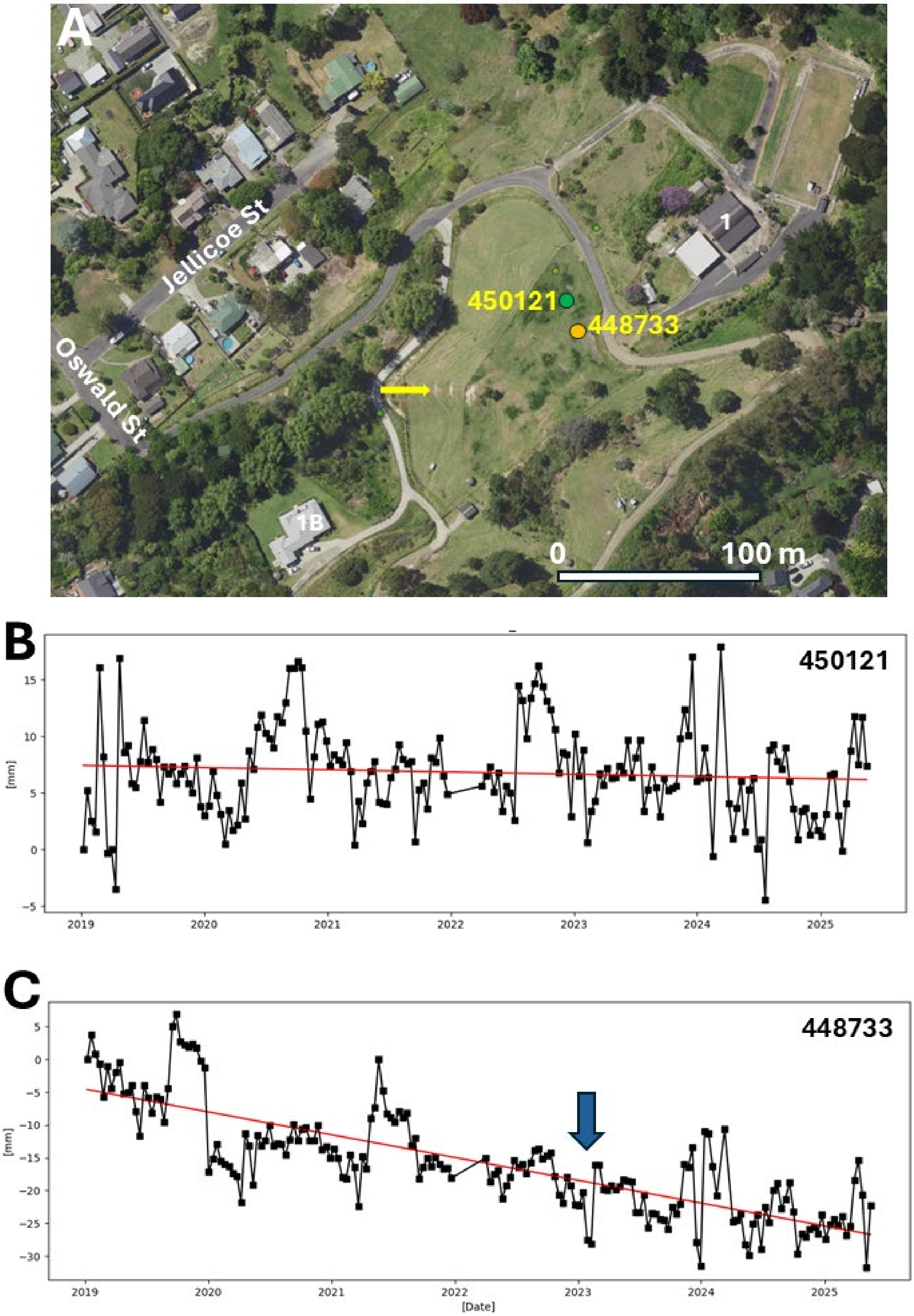

Figure 10: (A) Slopes above the east end of Oswald Street. Yellow arrow shows bulging of mid-slope; (B) Line-of-sight (LOS) velocity (mm/yr) time-series for point 450121; (C) Line-of-sight (LOS) velocity (mm/yr) time-series for point 448733. The points show contrasting velocity, showing deformation within the slope is segmented.

<u>Wallis Rd/SH35 new build area</u>

Figure 11 shows some example LOS velocity for slopes to the east of Wallis Road. Soils in the Wallis Road area of Gisborne is susceptible to landslides, as highlighted by Cook et al. (2022c). Since Cyclone Gabrielle, the land between Wallis Road and SH35 (Wainui Road) had undergone clearance and some earthworks, with the apparent aim of the landowners to undertake a residential subdivision on these sensitive soil slopes.

The geology in this part of Gisborne is Early Pleistocene Mangatuna Fm river and estuary deposits that have bene uplifted to form a plateau or terrace. This overlies the older Middle Miocene Tunanui Formation sandstones and mudstones of the Tolaga Gp, below. These units form the slopes below the reasonably flat plateau/terrace on which some houses have been built.

Figure 11 highlights 2 points around 611C Wainui Rd. This is right on the edge of the Mangatuna Fm plateau, with the ~35° slopes below on the Tolaga Gp soils. As can be seen from Figure 11B&C, significant long-term deformation is occurring here, and the LOS indicates similar slope velocity pre- and post- Cyclone Gabrielle. There is minimum set-back distance here from the top of the slope, with the plateau/terrace edge vulnerable to weathering.

Toe of Russell Street landslide - evidence of minor heave

Figure 12 is some example points at the toe of the Russell Street landslide. This landslide was active in the middle of 2023, and this led to several houses being removed from the slopes above the west end of Russell Street (Pola et al., 2025).

While the slope deformation to the west of Russell Street has been well documented, no deformation east of Russell Street has been delineated. Indeed, the slope deformation was thought to be limited to the slopes west of Russell Street, evident by increases velocity away from the sensor.

However, the LOS time series plots in Figure 12 show that there is evidence of deformation, but this is toward the sensor in the form of toe uplift (heave). Indeed, Figure 12B is the concrete pool surround at 198 Russell St, and this is showing gradual uplift (heave). Likewise, 10m to the northwest across Russell Street, the concrete blocks in the toe are also showing uplift (heave). While bulging and uplift in the mid-slope was reported by Pola et al. (2025), this is the first time clear evidence of toe uplift had been identified. Figure 13 is a field photo showing the deformed toe retaining blocks. Overall, the Mangatuna Fm and underlying Tolaga Gp soils represent a significant challenge for construction activities in Gisborne (Figure 14).

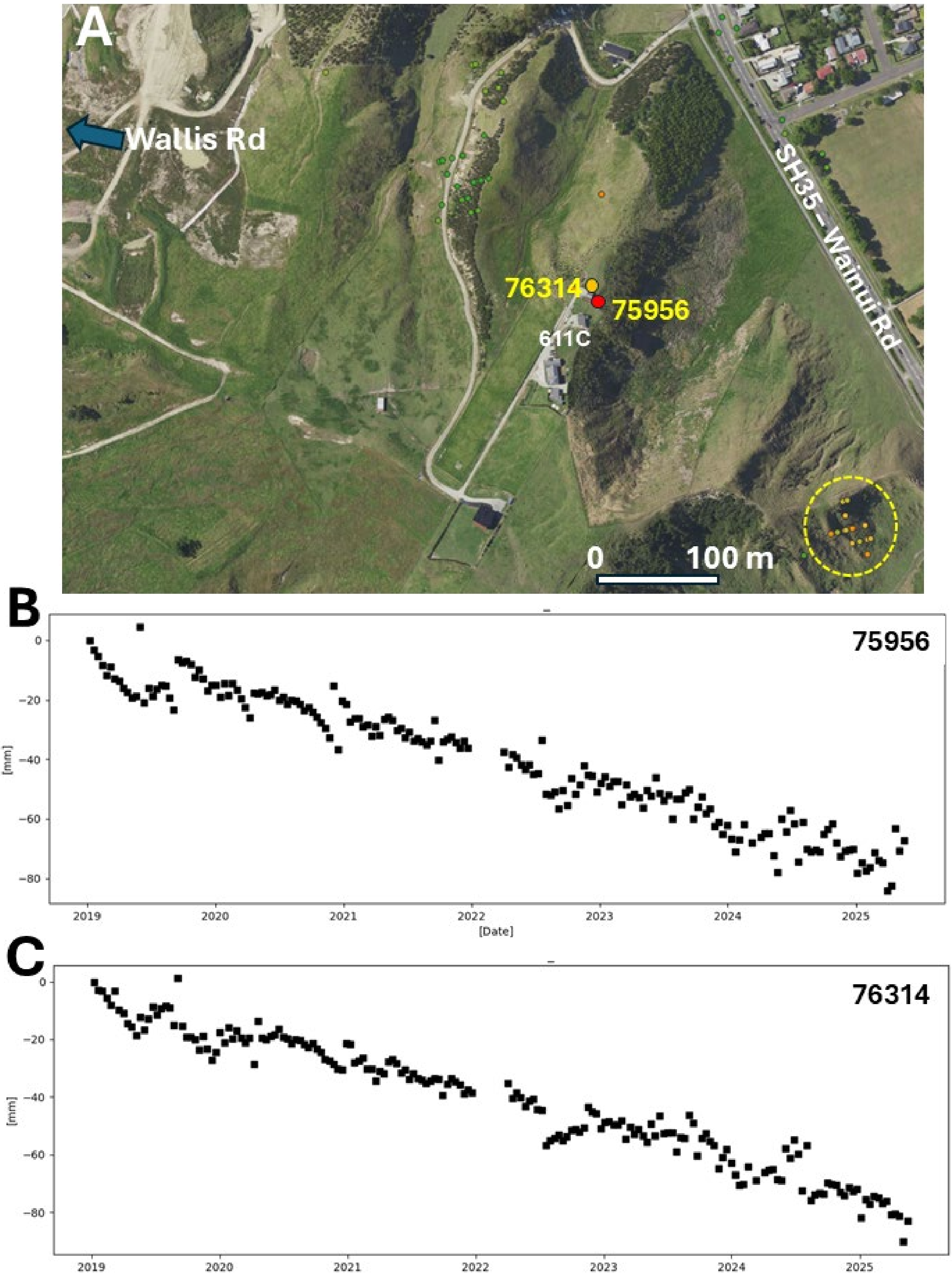

Figure 11: (A) Slopes between SH35 and the area of new land development east of Wallis Road; (B) point 75956 is right at the edge of the Mangatuna Formation cliff; (C) point 76314 is several meters back from the edge of the cliff, but still shows considerable movement. A cluster of movement on the slopes to the southeast is circled.

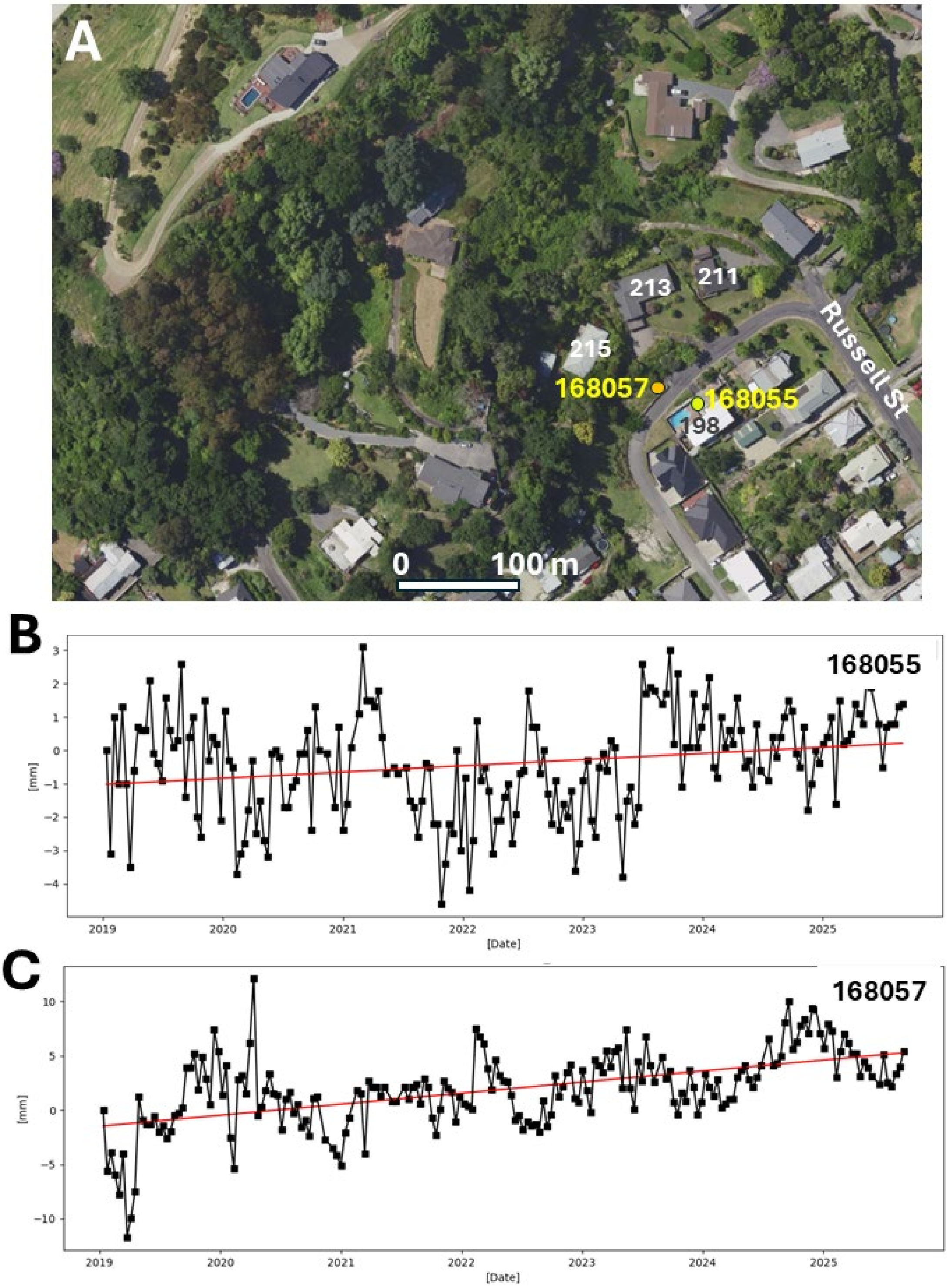

Figure 12: (A) Upward movement (heave) in the toe area of the Russell Street landslide (houses 213 & 215 have been removed since this image was taken); (B) point 168055 on retaining block at toe; (C) point 168057 at edge of 198 Russel Street's swimming pool.

Figure 13: Retaining blocks (1 m high) at toe of Russell St landslide, showing evidence of uplift (heave).

Figure 14: Edge of Pleistocene Mangatuna Fm plateau with Miocene Tolaga Gp below. These plateau remnants are highly unstable, as the Pleistocene soils become saturated and slump over the underlying impermeable mudstones.

Limitations and Future Work

Notwithstanding the above results, there are some key limitations that need to be acknowledged.

These limitations are as follows:

1. **Coherence loss in steep, vegetated escarpments limited PS-InSAR detection in some areas.** Coherence is a measure of the phase noise in the interferogram (the visual patterns in the stack of SAR images), and therefore is a measure of the reliability of the data. Coherence can be measured spatially, by measuring the stability of relationships between neighbouring pixels in the SAR images, and it can also be measured temporally by measuring the stability of a pixel over time. If corresponding pixels in image pairs are similar, correlation is high, and coherence is high. In contrast, if corresponding pixels in SAR image pairs are not similar, the phase will vary significantly, and coherence will be low (e.g. Lê et al., 2019).
2. **Reliance on descending Sentinel-1 imagery restricted displacement measurement to a single line-of-sight (LOS).** Only descending data was used, which is where the satellite is moving from the north pole to the south pole. This was because of the extremely large data files (terabytes) that need to be analysed. If ascending data (movement of the satellite from the south pole to the north pole) was also used, while this would have taken much longer to process, the combined dataset could have provided higher accuracy in detecting and measuring ground displacements. Also, combining both ascending and descending data can reduce geometric distortions. A geometric distortion is where the orientation of the topographic slope with respect to the satellite sensor is not ideal. For example, a south-facing slope is not ideal if only data from a descending satellite (i.e. north to south) orbit is used. In summary, the combination of ascending and descending InSAR data is a powerful tool (e.g. Barone et al., 2025) for enhancing the accuracy and reliability of various applications, particularly in the fields of geomatics and disaster management.
3. **Lack of GNSS or ground-based validation prevented independent confirmation of InSAR-derived displacement.** Occasionally, some InSAR studies have undertaken additional surveying of selected areas of their InSAR investigation using total stations and GNSS surveying techniques (Giorgini et al., 2026). This is to manually detect and map changes in the slope over time, and compare with the InSAR results. This can provide a very high precision validation of the InSAR results, but it is time consuming and is not spatially extensive (unlike InSAR), and so can only realistically provide a comparison over a small area of the InSAR survey area.

These limitations are consistent with challenges documented internationally in applying InSAR to landslide-prone, vegetated terrain.

Recommendations for future work are as follows:

1. Apply E-InSAR to parts of Auckland including Muriwai and Karekare to determine if this enhances coherence and characterisation of slope kinematics and resolution.
2. Integrate E-InSAR with GNSS and ground-based monitoring to provide independent validation of results.
3. Extend monitoring periods to capture long-term deformation trends and better distinguish seasonal signals from permanent slope movement.
4. Couple InSAR time-series with rainfall-threshold models to support early-warning systems.
5. Develop a national-scale InSAR monitoring programme, following international examples. This is now underway in New Zealand, led by GNS, via an MBIE Endeavour programme, "*Sliding Lands*".

Conclusions

Slope deformation is triggered by consecutive extreme rainfall events, and in some cases preceded or followed by measurable creep captured by InSAR. While coherence loss restricted coverage in some areas, PS-InSAR successfully detected slow deformation and seasonal cycles in peri-urban settings in Auckland.

In the Gisborne area, E-InSAR (combined PS and SBAS InSAR) was used to determine slope deformation. Downslope movement coincident with long-term slope failure was evident, as well as seasonal shrink-swell at some sites. At Russell Street landslide, toe uplift (i.e. movement toward the sensor) was evident. Taken together, there are all slope weathering processes that are typical in the region.

These findings confirm that InSAR is a useful monitoring tool in New Zealand, and can provide more valuable input when combined with LiDAR, rainfall data, and geomorphic analysis. By linking deformation rates with structural damage thresholds and integrating results with planning frameworks, this research demonstrates how satellite-based monitoring can support more resilient hazard management. Broader adoption of InSAR, embedded within land-use planning, would enhance the ability of councils and government agencies to identify at-risk slopes and reduce exposure, thereby supporting safer, more resilient communities.

Publications, communications and engagement

Akhtar W, Brook M, Tunnicliffe J, Cook M, Cave M. (2026). Landscape sensitivity and change in the Gisborne region of New Zealand. *11th International Conference on Geomorphology*, Christchurch, 2-6 February.

Brook M (2024) *Building Act is preventing full hazard zoning improvements* https://newsroom.co.nz/2024/02/13/the-building-act-is-preventing-full-hazard-zoning-improvements/

Brook M, Le Cheminant H, Akhtar W, Cook M. (2025). Recent landslides in Auckland, New Zealand: InSAR investigation and material properties. *STAR conference*, Suva, 26-28 November.

Codyre SV (2024). *Identifying and assessing landslide susceptibility in Tairawhiti Gisborne after Cyclone Gabrielle: insights from InSAR and remote sensing*. Unpublished BSc Hons dissertation, University of Auckland.

Le Cheminant HJ (2025). *Investigating slow-moving landslides in the Auckland region using LiDAR and Sentinel-1 InSAR*. MEngGeol thesis, University of Auckland.

Le Cheminant H, Pickering C, Cook M, Brook M. (2026). Landscape sensitivity to rainfall triggering effects: western Auckland, New Zealand. *11th International Conference on Geomorphology*, Christchurch, 2-6 February.

Pola A, Brook MS, Cook M, Wotherspoon L, Cave M. (2025). Understanding selective triggering of landslide movement in response to rainfall, Gisborne, New Zealand. *New Zealand Journal of Geology and Geophysics*, 68(5), 1064–1080.

References

Abazu G, Brook MS, Druskovich B, Brideau M-A, Hayward BW. (2025). Rainfall-triggered landslides from the January 2023 1-in-200 year storm at Maungakiekie/One Tree Hill, Auckland, New Zealand. New Zealand Journal of Geology and Geophysics, 68(5), 1049–1063.

Barone A, Fedi M, Pepe A. et al. (2025). Inferring 3D displacement time series through InSAR measurements and potential field theory in volcanic areas. Scientific Reports, 15, 4719.

Brook M. (2023). How to prevent building where it isn't safe. Bulletin of the Greek Society of Soil Mechanics and Geotechnical Engineering, 172, 3-4.

Brook MS, Nicoll C. (2024). Brief report of fatal rainfall-triggered landslides from record-breaking 2023 storms in Auckland, New Zealand. Landslides, 21, 1581-1589.

Closson D, Milisavljevic N. (2017). InSAR Coherence and Intensity Changes Detection. In: Beumier C et al. (eds), Mine Action - The Research Experience of the Royal Military Academy of Belgium. InTechOpen, Zagreb. Chapter 6.

Cook M, Brook M, Cave M, Wolter A, Rosser B. (2022a). November 2021 rainfall-triggered landslides in Gisborne/Tairāwhiti: field reconnaissance and insights from InSAR monitoring. New Zealand Geomechanics, 104. 46-57.

Cook ME, Brook MS, Hamling IJ, Cave M, Tunnicliffe JF, Holley R, Alama D. (2022b). Engineering geomorphological and InSAR investigation of an urban landslide, Gisborne, New Zealand. Landslides, 19, 2423–2437.

Cook M, Brook MS, Tunnicliffe J, Cave M., Gulick N (2022c). Preliminary investigation of emerging suburban landsliding in Gisborne, New Zealand. Quarterly Journal of Engineering Geology and Hydrogeology, 55(3) https://doi.org/10.1144/qjegh2021-087

Cook M, Brook M, Cave M. (2023a). Interferometric Synthetic Aperture Radar (InSAR) and field-based observations of rainfall-triggered landslides from the November 2021 storm, Gisborne/Tairāwhiti, New Zealand. New Zealand Geographer, 79, 138-152.

Cook ME, Brook MS, Hamling IJ, Cave M, Tunnicliffe JF, Holley R. (2023b). Investigating slow-moving shallow soil landslides in a vulnerable city using Sentinel-1 InSAR data. Landslides, 20, 427-446.

Despojo J, Brook MS, Alama D, Cook ME, Cave M. (2025). Landslide preparation by forestry activity in a region of high erosion rates: Waingake Landslide, northeast New Zealand. New Zealand Journal of Geology and Geophysics, 68(5), 1015–1030.

Ferretti, A. (2014). Satellite InSAR data: Reservoir monitoring from space (1st ed., EET 9). EAGE.

Giorgini E, Lazecky M, Hooper A, Gandolfi S. (2026). Best Practice for Integrating InSAR and GNSS Observations in High-Density GNSS Networks. IEEE Journal of Selected Topics in Applied Earth Observations and Remote Sensing, doi: 10.1109/JSTARS.2026.3675875

Howard ME, Hunter AJ, Roberts RC, Brook MS (2025). Landslide hazard and loss-of-life risk assessment for Muriwai, New Zealand following Cyclone Gabrielle in February 2023. New Zealand Journal of Geology and Geophysics, 68(5), 1031–1048.

Hussain S et al. (2025). Integrated PSInSAR and SBAS-InSAR analysis for landslide detection and monitoring. Physics and Chemistry of the Earth, Parts A/B/C. 139:103956. https://doi.org/10.1016/j.pce.2025.103956

Lê TT, Froger J-L, Hrysiewicz A, Paris R. (2019). Coherence Change Analysis for Multipass Insar Images Based on the Change Detection Matrix. IGARSS 2019 - 2019 IEEE International Geoscience and Remote Sensing Symposium, Yokohama, Japan, p. 1518-1521, doi: 10.1109/IGARSS.2019.8898723.

Notti D, Herrera G, Bianchini S, Meisina C, García-Davalillo JC, Zucca F (2014). A methodology for improving landslide PSI data analysis. International Journal of Remote Sensing 35(6): 2186–2214.

Pola A, Brook MS, Cook M, Wotherspoon L, Cave M. (2025). Understanding selective triggering of landslide movement in response to rainfall, Gisborne, New Zealand. New Zealand Journal of Geology and Geophysics, 68(5), 1064–1080.

SARScape (2025). SARscape Version 6.1.0.

Solari, L., Del Soldato, M., Raspini, F., Barra, A., Bianchini, S., Confuorto, P., et al. (2020). Review of satellite interferometry for landslide detection in Italy. Remote Sensing, 12(8), 1351.

Appendix 1 – Coherence and confidence in the results

Although InSAR results rarely present or quantify uncertainty in a formal sense (e.g. error bars or confidence intervals), uncertainty is dealt with implicitly through how the data is processed and then framed and interpreted. Coherence is the main way that uncertainty is constrained and quantified. It is succinctly summarised by Closson and Milisavljevic (2017, p. 162-163).

SAR repeat pass interferometry is based on two image acquisitions of the same area from slightly displaced orbits of the satellite. The Sentinel repeat pass is typically 12 days. During the processing, both images are coregistered. The phase differences are calculated, creating interferograms. These interferograms contain information related to local elevation, local displacement, and noise. This noise, or phase decorrelation, records the slight changes in scatterers distribution on the observed Earth surface between the two acquisitions.

One of the "interferometric products" from two SAR scenes is a coherence image that presents the confidence level of each pixel in the phase difference image. Coherence (equation below) refers to a fixed relationship between waves in a beam of electromagnetic radiation. Two wave trains are "coherent" when they are in phase. In SAR interferometry, coherence is used to describe systems that preserve the phase of the received signal. The coherence value can be estimated by means of the "local coherence" of an interferometric SAR image pair. The local coherence estimator is the cross-correlation coefficient of the couple estimated on a small window:

$$\gamma \cong \frac{\left|\sum_{i=1}^{L}\sum_{j=1}^{M}\mathrm{Im}_1\left(x_i,z_j\right)\mathrm{Im}_2^*\left(x_i,z_j\right)\right|}{\sqrt{\sum_{i=1}^{L}\sum_{j=1}^{M}\left|\mathrm{Im}_1\left(x_i,z_j\right)\right|^2\sum_{i=1}^{L}\sum_{j=1}^{M}\left|\mathrm{Im}_2\left(x_i,z_j\right)\right|^2}}$$

where Im_1 is the complex signal of the "master" image and Im^*_2 is the complex signal in the "slave" image. The coherence of a pixel is estimated by the means of kernels with $L \times M$ pixels. In an interferogram, the coherence ranges from 0.0 (total decorrelation, the interferometric phase is pure noise) to 1.0 (phase correlation is preserved). As a statistical value, it cannot provide quantitative measurements of the ground scatterers disturbances. However, a physical interpretation is that it represents the fraction of power scattered by unchanged parts of the scene. The coherence image serves as a measure of the quality of an interferogram and gives information about the surface type (e.g., vegetated versus soil and rock) or shows when a tiny, otherwise invisible change has occurred in the image. Coherence imagery is able to detect centimeter scale changes in the scatterers distribution.

In summary, as a statistical value, coherence cannot provide quantitative measurements of the ground scatterers disturbances. However, a physical interpretation is that it represents the fraction of power scattered by unchanged parts of the scene.

Appendix 2 Integrated PS and SBAS InSAR workflow example ("E-SBAS") InSAR

The flow diagram below shows example methodology workflow for enhanced E-InSAR processing (i.e. combined PS and SBAS InSAR), from SARScape (2025). Note that SBAS InSAR on its own was previously applied successfully to the Gisborne area by Cook et al. (2023b) for the period 2016-2021.

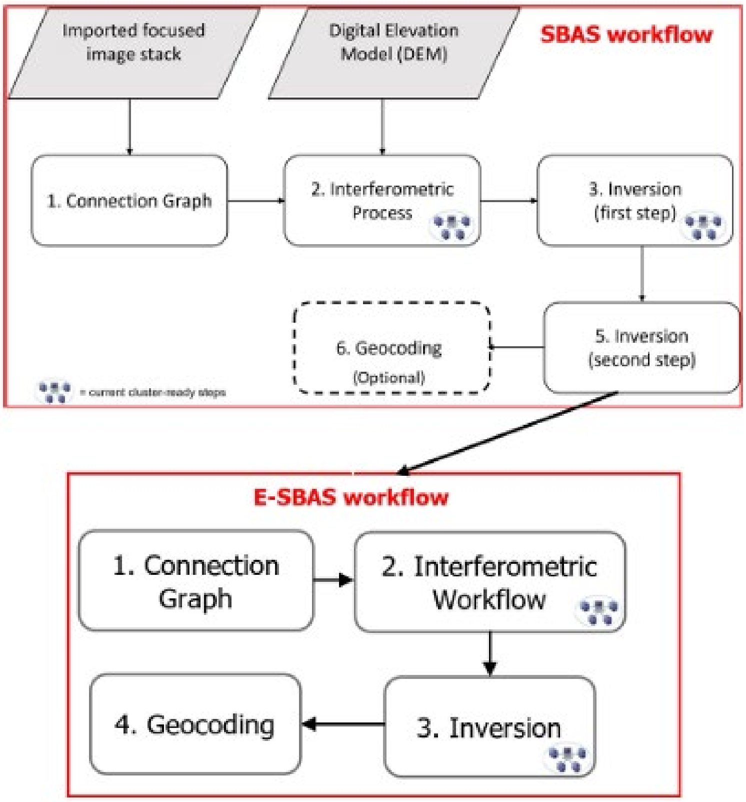

Figure 1 E-SBAS block diagram